Phase transition in two dimensions far from thermal equilibrium

Patrick Dillmann,[1] Georg Maret,[1] and Peter Keim[1]
[1] *University of Konstanz, D-78457 Konstanz, Germany*
(Dated: March 28, 2013)

A two-dimensional monolayer of monodisperse colloids is quenched rapidly below the melting temperature into the crystalline phase and the nature of the transition is investigated. Analyzing the local order as function of time we find shortly after the quench a bimodal distribution of highly ordered (crystalline) and fluidlike particles, indicating that the KTHNY-scenario known from 2D equilibrium transitions does not hold. Critical nucleation theory can not describe the solidification scenario found in our experiment, either, as we do not find a lag time nor a critical nucleus size. The average size of nuclei grows monotonically as expected, but surprisingly, comparing the size of an individual 'nucleus' in consecutive timesteps, shrinking is always more probable than growing. This indicates a strongly asymmetric nucleation behaviour. Nevertheless, the averaged dynamics of the degree of crystallinity is found to be in very good agreement with the heuristic Johnson-Mehl-Avrami-Kolmogorov (JMAK)-scenario.

PACS numbers: 05.70.Fh, 05.70.Ln, 64.60.Q-, 64.70.pv, 82.70.Dd

Crystal nucleation is one of the basic physical phenomena that govern the growth and the structure of any crystalline state in three dimensions. Therefore this topic [1–15] is one of the most important and interesting areas of condensed matter physics. Although it is rather easy to control the crystal nucleation process empirically, understanding this phenomenon at the fundamental level has been a great challenge for many decades. The most widely used concept, the Classical Nucleation Theory (CNT), attempts to describe this complex process by treating the nuclei as compact spheres that grow if their size exceeds a critical value [1–3]. This critical value is determined by a maximum in the free energy, where the energy gain in the volume $\sim r^3$ overcompensates the surface energy cost $\sim r^2$ of the nucleus. Colloidal systems, where micrometer sized particles are dispersed in a solvent, allow to investigate such nucleation on a single particle level. Depending on interaction strength and volume fraction of the colloids in the solvent, different thermodynamic phases like crystalline, fluid, gaslike and (in two dimensions) hexatic phases can be identified. Colloids are small enough to undergo Brownian motion and can be described as a statistical ensemble but they are large enough to be monitored with optical methods like light scattering or (confocal) video microscopy. But not only the structure can be monitored on an 'atomistic' scale. Since the particle dynamic scales inversely with the size of the particles, structural rearrangements like phase transitions can be monitored on single particle level on almost all relevant time scales.

However, experiments on hard sphere colloidal systems [7, 8, 11], where individual particle interactions are sufficiently simple to be modeled theoretically differ from the predictions of critical nucleation theory. In more complex systems, the CNT calculation underestimates the nucleation rate by many orders of magnitude [16]. It is obvious that the simple picture of a spherical seed has to be extended. In computer simulation studies of hard sphere colloidal systems in 3D [17], and for phase-field-crystal calculations in 2D [18], a precursor-mediated two-step crystallization was observed. Dense amorphous clusters are formed as the first step and then those clusters act like precursors for the nucleation of well-ordered crystallites. In experiments in 2D with effective attractive interactions between particles such precursors are found [19, 20], too, but might be explained with sublimation rather than nucleation. Dusty plasma experiments in 2D showed a power-law increase of average crystallite domain size as measured by bond-order correlation length [21] and microheterogeneity in structural evolution [22].

It is well known that dimensionality affects phase transitions. Whereas nucleation of supercooled fluids in three dimension is a first order phase transition including phase equilibrium, the melting process in a two-dimensional system in equilibrium has been a matter of debate for long. While Kosterlitz and Thouless proposed a continuous transition induced by topological defects like dislocations at the melting temperature T_m [23, 24], Chui later argued for a first order transition similar to the case in three dimensional systems [25]. Here, the symmetry is restored in the high temperature phase by the spontaneous generation of grain boundaries. The presence of a hexatic phase, an intermediate phase between the isotropic liquid and the crystalline state, was predicted by Nelson and Halperin [26, 27], as extension of the theory by Kosterlitz and Thouless. The hexatic phase is an anisotropic fluid and a second type of topological defects, namely disclinations, are needed to restore isotropy at a higher temperature T_i. Young independently calculated the critical exponents at the melting temperature T_m [28]. As colloidal systems are excellent model systems to observe phase transitions, experiments have been done on 2D or quasi-2D colloidal systems using optical microscopy with video imaging [29–33] to verify the

predicted two step transition and the existence of a hexatic phase. In [34, 35] we were able to investigate the microscopic mechanism of the so-called KTHNY-theory based on defect unbinding. The critical exponents of diverging length scales are in agreement with renormalization group calculations. In heating and cooling cycles we found the KTHNY-picture to hold as melting and freezing scenario without hysteresis of the transition points, but care has to be taken that the system is always in thermal equilibrium. We did not observe a phase equilibrium or other first order signatures and accordingly we identified the transitions to be continuous.

Here, we present a study of solidification far from thermal equilibrium. If the system is quenched rapidly at ultra-short timescales from the isotropic fluid phase into the crystalline phase the scenario alters completely: we did NOT observe the two distinct phase transitions and the intermediate hexatic phase [36]. If quenched rapidly, the system solidifies into a poly-crystalline sample. We investigate this phase transition far from thermal equilibrium on single particle level and show that critical nucleation theory does not describe the phenomena observed.

The 2D colloidal monolayer is realized out as follows. A droplet of a suspension composed of polystyrene spheres dispersed in water is suspended by surface tension in a top sealed cylindrical hole ($\varnothing = 6\ mm$) of a glass plate. The particles are 4.5 μm in diameter and have a mass density of 1.5 g/cm^3 leading to sedimentation. The large density is due to the fact that the polystyrene beads are doped with iron oxide nanoparticles leading to superparamagnetic behavior. After sedimentation particles are arranged in a monolayer at the planar and horizontal water-air interface of the droplet and hence form an ideal 2D system. Particles are small enough to undergo Brownian motion but large enough to be monitored with video-microscopy. An external magnetic field H perpendicular to the water-air interface induces a magnetic moment in each bead (parallel to the applied field) leading to repulsive dipole-dipole interaction between all particles. We use the dimensionless control parameter Γ to characterize this interaction strength; it is given by the ratio of dipolar magnetic to thermal energy

$$\Gamma = \frac{\mu_0}{4\pi}\frac{(\chi H)^2(\pi\rho)^{3/2}}{k_B T} \propto T_{sys}^{-1} \qquad (1)$$

and thus can be regarded as an inverse system temperature. The state of the system in thermal equilibrium - liquid, hexatic or solid - is solely defined by the strength of the magnetic field H since the temperature T, the 2D particle density ρ and the magnetic susceptibility per bead χ are kept constant experimentally. In these units the melting temperature (crystalline - hexatic) is at about $\Gamma = 60$ and the transition from hexatic to isotropic at about $\Gamma = 57$. Based on an equilibrated liquid system ($\Gamma \approx 15$) [37] we initiate a temperature jump with cooling rates up to $d\Gamma/dt \approx 10^4\ s^{-1}$ into the crystalline region of the phase diagram $\Gamma_M \geq 60$ [34, 35]. This temperature quench triggers a crystallization process in the system where the time scale of cooling is 10^5 faster compared to the intrinsic Brownian timescale $\tau_B = 50$ sec, i.e. the time particles need to diffuse the distance of their own diameter. An elaborate description of the experiment can be found in [38]. The field of view is $1160 \times 865\ \mu m^2$ in size and contains about 9000 colloids. Each temperature quench to the same final value of the control parameter Γ_F is repeated at least ten times with sufficient equilibration times in between and all analyzed quantities are averaged by the number of repetitions of the quenches.

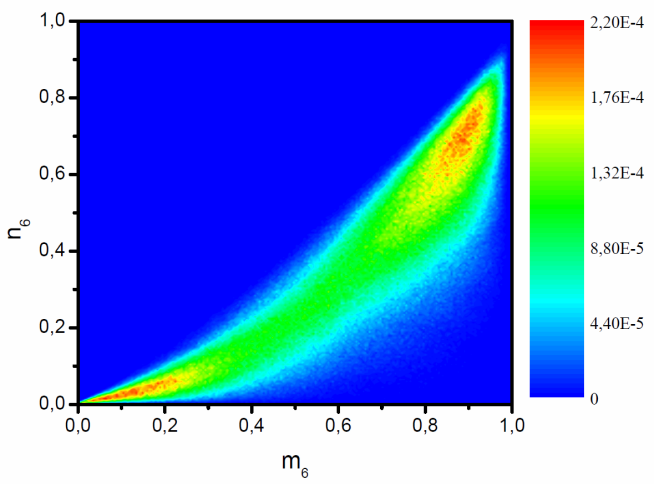

FIG. 1. The color code measures the frequency of locally ordered particles in the m-n-plane 220 s after a (inverse) temperature quench from $\Gamma = 13$ (deep in the fluid phase) to $\Gamma = 63$ in the crystalline stage. A bimodal distribution of crystalline-like particles with high local order (upper right corner) and fluid-like particles with low local order (lower left corner) is found.

To analyze the degree of local order after a temperature quench we use a criterion based on the magnitude $m_{6_k} = |\psi_k|$ of the local bond order parameter [39], where the local bond order field is given by

$$\psi(\vec{r}) = \psi_k = \frac{1}{N_j}\sum_j e^{i6\theta_{jk}} \qquad (2)$$

Here the sum runs over the N_j next neighbors of the particle k at position $\vec{r}$ and θ_{jk} is the angle between a fixed reference axis and the bond of the particle k and its neighbor j. For particle k, m_{6_k} is close to one if the neighboring particles are sitting on a hexagon and close to zero if the neighboring particles are not sixfold. One can sharpen this measure of local sixfold symmetry by taking the magnitude of the projection of ψ_k

$$n_{6_k} = |\psi_k^* * 1/N_l \sum_l \psi_l| \qquad (3)$$

to the mean local orientation field given by the nearest neighbours. It takes the second nearest neighbors into

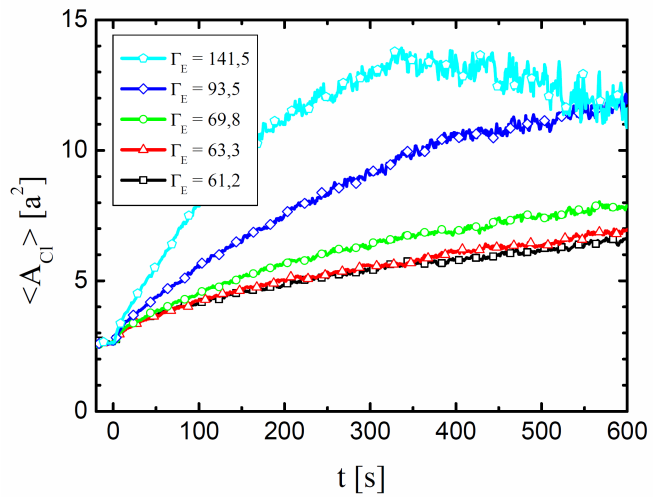

FIG. 2. Average size of the nuclei (in units of the voronoi-cell of individual particles) for five different quench depth as function of time. The nonmonotonic behavior of the deepest quench is an artefact, since (large) crystallites which exceeds the field of view are ignored. Note, that nucleation starts immediately after the quench.

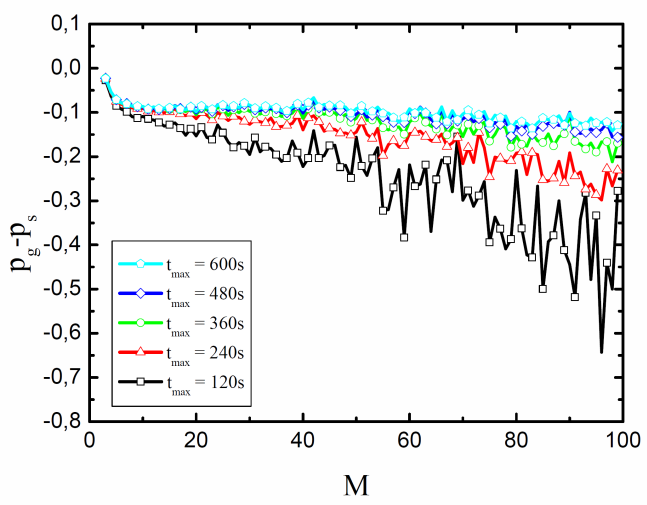

FIG. 3. The shrinking probability after a quench (here $\Gamma_F = 93.5$ is shown) for a crystalline cluster composed of M particles is always larger than the growing probability. Unlike in 3D systems one can not determine a critical nucleus size on single particle level and hence 2D systems out of equilibrium can not be described with critical nucleation theory. Solidification is strongly affected by order fluctuations and shrinking and growing appear to be quite asymmetric.

account and determines how the orientation of particle k fits into the orientation of its neighboring particles. Fig. 1 shows the probability distribution in the m_6-n_6-plane. The color code measures how often a particle with high or low local order is found. Compared to the melting scenario in thermal equilibrium, where only a unimodal distribution is found [35, 40], one can clearly identify a bimodal distribution compatible with a nucleation scenario. To investigate the time dependence of growing grains, we define a particle to be part of a crystal cluster if the following three conditions are fulfilled for the particle itself and at least one nearest neighbour: a) The magnitude of the local bond order field m_{6_k} must exceed 0.6 for both neighboring particles. b) The bond length deviation $\Delta|l_{kl}|$ of neighboring particles k and l is less than 10% of the average particle distance l_a. c) The variation in bond orientation $\Delta\Theta = |\psi_k - \psi_l|$ of neighboring particles k and l must be less than 2.3° in real space (less than 14° in sixfolded space). The threshold values are defined in comparison with mono-crystalline and isotropic fluid phases under equilibrium conditions and the qualitative results are robust to (moderate) variations (about ±20%) of the threshold values. Simply connected domains of particles which fulfill all three criteria are merged to a crystalline cluster. Comparing our results with [17–20], no amorphous precursors with increased density are found in our experiment. Analyzing crystalline and fluidlike domains the 2D density measured by Voronoi-cells is identical within the error bar. Figure 2 shows the average size of the crystalline cluster up to 10 min after the quench. As expected, the average size of the nuclei grows monotonically as function of time, for all quench depths ranging from quenches close to the melting temperature Γ_m to quenches deep in the crystalline phase. We checked that the maximum in size for the quench to $\Gamma = 141$ is an artefact since only crystallites being completely in the field of view are counted. For this deepest quench some crystallites grow beyond the field of view after about 5 min and are ignored when determining the mean size. It is important to note that the nucleation starts immediately after the quench such that no lag time of critical nucleation is detectable. Additionally, with the parameters given above about 10% of the particles are identified as crystalline before the quench, deep in the fluid phase at $\Gamma = 13,7$. Such a precritical nucleus consists in average of 2.7 particles and the lifetime is a few seconds. The large amount (compared to 3D systems) of precritical nuclei is due to the fact that the preferred local symmetry in 2D is sixfold, both in the crystalline as well as fluid phase. (If the criteria for crystalline particles are tightened, the amount of precritical nuclei decreases but then a monocrystal in equilibrium is not detected as such any more). This already indicates that the formation of a nucleus in 2D after a temperature quench is not a rare event and the critical nucleation barrier is very low. In other words, the size of a critical nucleus consists of two particles, being the smallest possible cluster. In this case one would expect all individual nuclei ≥ 2 particles to grow after the quench which is surprisingly not the case. In Figure 3 the difference of growing p_g and shrinking probability p_s of nuclei is plotted for different time windows after a quench to $\Gamma_F = 93.5$

where M is the size of the nuclei given by the number of the particles which belong to the cluster. The probability for shrinking and growing for individually labeled clusters of size M is given by $p_{g/s} = N_{g/s}/N_M$ where N_M is the number of clusters of size M and N_g or N_s are the numbers of those clusters which are larger $M_\tau > M$ or smaller $M_\tau < M$ after a finite waiting time τ.

For all time windows and nucleus sizes the probability of shrinking is larger than the probability of growing. This is true for all quench depths performed, close to melting ($\Gamma_F = 61$) as well as deep into the crystalline phase ($\Gamma_F = 141$, not shown here). The waiting time was varied over almost two decades from $0.1 - 10$ sec and no qualitative differences were found. Obviously shrinking (often, but small areas) and growing (less often, but larger areas) is quite asymmetric and the nucleation process far from equilibrium is strongly dominated by fluctuations. Practically all grains which are present during the quench disappear again. Two mechanisms appear to be responsible for this. First, small grains dissolve completely into fluidlike particles and second, grains of intermediate size fluctuate strongly in orientation such that they disrupt into smaller subdomains. Such subdomains frequently merge again but then the net contribution to the growing probability is typically zero, since one grain has grown but the other(s) has/have 'disappeared'. Interestingly the lifetime of crystalline clusters after the quench is again a few seconds and comparable to the lifetime of 'subcritical nuclei' before the quench.

To further analyze the crystallization dynamics we do not measure the size of individual grains but determine the overall fraction of crystalline particles as function of time $X(t) = \frac{N^{X-tal}(t)}{N(t)}$ where $N^{X-tal}(t)$ is the number of crystalline particles and $N(t)$ is the number of all particles in the field of view at time t. Following a heuristic description of nucleation introduced by Johnson-Mehl-Avrami-Kolmogorov (JMAK-theory) the rate of crystallinity can be described with

$$X(t) = 1 - e^{-k(t-t_0)^n} \tag{4}$$

if the following criteria are fulfilled: i) Nucleation occurs randomly and homogeneously over the entire untransformed portion of the material. ii) Growth occurs at the same rate in all directions. iii) The growth rate does not depend on the extent of transformation [41–43]. Whereas the first two criteria are reasonable, the last is complied since our system is not transport limited (the area density of fluidlike and crystalline particles is the same).

Figure 4 shows the degree of crystalline particles as function of time. Solids lines are a fit to Eqn. 4 where the parameter t_0 accounts for the 10% particles being already crystal-like in structure before the quench. Very good agreement is found and by taking twice the logarithm of Eqn. 4 one can extract the Avrami-exponent (see inset).

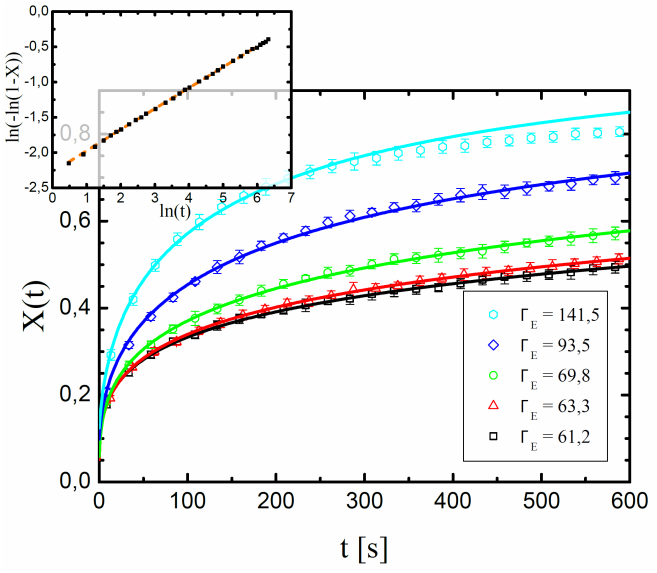

FIG. 4. Fraction of crystalline particles for different quench depths. The solid lines are fits to Eqn. 4. The inset shows an Avrami-plot for $\Gamma_E = 61.2$ to determine the exponent n in Eqn. 4 from the slope of the curve.

Γ_F	k	t_0 $[s]$	n
61.2	0.1 ± 10^{-7}	0.09 ± 10^{-3}	0.29 ± 10^{-7}
63.3	0.1 ± 10^{-5}	0.13 ± 10^{-3}	0.31 ± 10^{-5}
69.8	0.09 ± 10^{-7}	0.28 ± 10^{-3}	0.35 ± 10^{-7}
93.5	0.09 ± 10^{-6}	1.27 ± 10^{-3}	0.4 ± 10^{-6}
141	0.1 ± 10^{-4}	1.7 ± 10^{-4}	0.45 ± 10^{-6}

Whereas the parameter k is independent of the quench depth, the Avrami-exponent increases monotonically with the quench depth but is always smaller than unity.

In conclusion, we found that neither the KTHNY-scenario nor critical nucleation does describe the phenomena observed for this 2D non-equilibrium scenario [44]. There is evidently no nucleation barrier since a) nucleations starts immediately after the quench and no lag time is observable, b) the density of nucleation centers is too large for a nucleus to be a rare event, and c) the growing probability is always negative, independent of the size of the nucleus. Nuclei which appeared immediately after the quench usually disappear again, almost none of them will grow to a domain in the polycrystal since the local order fluctuates strongly. Quantitative agreement with the heuristic Johnson-Mehl-Avrami-Kolmogorov description is observed and even for the deepest quench we did never observe an amorphous phase. We hope our work will stimulate theory and simulations to investigate such novel phenomena observed in phase transitions far from thermal equilibrium.

We acknowledge financial support from the German Research Foundation (DFG), SFB-TR6 project C2.

[1] R. Becker, W. Döring: *Ann. Phys.*, **24**, 719 (1935)
[2] D. Turnbull, J.C. Fisher: . *J. Chem. Phys.*, **17**, 71 (1949)
[3] C.S. Kiang, D. Stauffer, G.H. Walker, O.P. Puri, J.D. Wise Jr., E.M. Patterson: *J. Atmos. Sci.*, **28**, 1222 (1971)
[4] K. Binder, D. Stauffer: *Adv. Phys.*, **25**, 343 (1976)
[5] D.W. Heermann, W. Klein: *Phys. Rev. Lett.*, **50**, 1062 (1983)
[6] P.N. Pusey, W. van Megen: *Nature*, **320**, 340 (1986)
[7] J. Zhu, M. Li, R. Rogers, W. Meyer, R.H. Ottewill, STS-73 Space Shuttle Crew, W.B. Russel, P.M. Chaikin: *Nature*, **387**, 883 (1997)
[8] U. Gasser, E.R. Weeks, A. Schofield, P.N. Pusey, D.A. Weitz: *Science*, **292**, 258 (2001)
[9] U. Gasser, A. Schofield, D.A. Weitz: *J. Phys. Cond. Mat.*, **15**, 375 (2003)
[10] S. Auer, D. Frenkel: *Nature*, **409**, 1020 (2001)
[11] V.J. Anderson, H.N. Lekkerkerker: *Nature*, **416**, 811 (2002)
[12] S. Auer, D. Frenkel: *Adv. Polym. Sci.*, **173**, 149 (2005)
[13] D. Moroni, P.R. ten Wolde, P.G. Bolhuis: *Phys. Rev. Lett.*, **94**, 235703 (2005)
[14] A. Cacciuto, S. Auer, D. Frenkel: *Nature*, **428**, 404 (2004)
[15] L. Zheng, Q. An, Y. Xie, Z.H. Sun, S.N. Luo: *J. Chem. Phys.*, **127**, 164503 (2007)
[16] V.I. Kalikmanov, J. Wlk, T. Kraska: *J. Chem. Phys.*, **128**, 124506 (2008)
[17] T. Schilling, H. J. Schöpe, M. Oettel, G. Opletal, I. Snook: *Phys. Rev. Lett.*, **105**, 025701 (2010)
[18] L. Granasy, G. Tegze, G.I. Toth, P. Tamas: *Phil. Mag,*, **91**, 123 (2011)
[19] T.H. Zhang, X.Y. Liu: *J. Am. Chem. Soc.*, **129**, 13520 (2007)
[20] J.R. Savage, A.D. Dinsmore: *Phys. Rev. Lett.*, **102**, 198302 (2009)
[21] P. Hartmann, A. Douglass, J.C. Reyes, L.S. Matthews, T.W. Hyde, A. Kovacs, Z. Donko: *Phys. Rev. Lett.*, **105**, 115004 (2010)
[22] Chi Yang, Chong-Wai Io, Lin I: *Phys. Rev. Lett.*, **109**, 225003 (2012)
[23] J.M. Kosterlitz, D.J. Thouless: *J. Phys. C*, **5**, 124 (1972)
[24] J.M. Kosterlitz, D.J. Thouless: *J. Phys. C*, **6**, 1181 (1973)
[25] S.T. Chui: *Phys. Rev. B.*, **28**, 178 (1983)
[26] B.I. Halperin, D.R. Nelson: *Phys. Rev. Lett.* **41**, 121 (1978)
[27] D.R. Nelson, B.I. Halperin: *Phys. Rev. B.*, **19**, 2457 (1979)
[28] A.P. Young, *Phys. Rev. B*, **19**, 1855 (1979)
[29] C.A. Murray, D.H. Van Winkle: *Phys. Rev. Lett.*, **58**, 1200 (1987)
[30] Y. Tang, A.J. Armstrong, R.C. Mockler, W.J. O'Sullivan: *Phys. Rev. Lett.*, **62**, 2401 (1989).
[31] R.E. Kusner, J.A. Mann, J. Kerins, A.J. Dahm: *Phys. Rev. Lett.*, **73**, 3113 (1994)
[32] A.H. Marcus, S.A. Rice: *Phys. Rev. Lett.*, **77**, 2577 (1996)
[33] K. Zahn, R. Lenke, G. Maret: *Phys. Rev. Lett.*, **82**, 2721 (1999)
[34] H.H. von Grünberg, P. Keim, K. Zahn, G. Maret: *Phys. Rev. Lett.*, **93**, 255703 (2004)
[35] P. Keim, G. Maret, H.H. von Grünberg: *Phys. Rev. E*, **75**, 031402 (2007)
[36] P. Dillmann, P. Keim, G. Maret: *J. Phys. Cond. Mat.*, **20**, 404216 (2008)
[37] The equilibration time to gain a completely flat water/air interface without any gradient of particle numberdensity within the plane is several weeks up to a few month.
[38] F. Ebert, P. Dillmann, G. Maret, P. Keim: *Rev. Sci. Inst.*, **80**, 083902 (2009)
[39] A.E. Larsen, D.G. Grier: *Phys. Rev. Lett*, **76**, 3862 (1996)
[40] P. Dillmann, G. Maret, P. Keim: *Jour. Phys. Cond. Mat.* **24**, 464118 (2012)
[41] A.N. Kolmogorov: *Izv. Akad. Nauk. SSSR Ser. Mat.* **1**, 355 (1937)
[42] W.A. Johnson, R.F. Mehl: *Trans. Am. Inst. Min. Metall. Eng.*: **135**, 416 (1939)
[43] M. Avrami: *J. Chem. Phys.* **7**, 1103 (1939)
[44] Using topological measures like pair distribution function and minkowski functionals of the spatial nuclei distribution we did not find a typical lenght scale compatible with spinodal composition.